PROCEEDINGS OF THE SOCIETY FOR EXPERIMENTAL BIOLOGY AND MEDICINE **188**, 159–168 (1988)

An Immunocytochemical Method for Quantification of Lung Tissue Fibronectin (42722)

YVONNE M. BELLAY,* ANNE M. DAYER,* JEFFREY E. GROSSMAN,†‡ AND JAMES A. WILL*‡

Department of Veterinary Science, University of Wisconsin, Madison, Wisconsin 53706; Departments of †Medicine and ‡Anesthesiology, University of Wisconsin, Madison, Wisconsin 53792

Abstract. A technique to quantify tissue fibronectin was developed, using peroxidase–antiperoxidase immunocytochemistry and automated scanning light microscopy. This technique was developed using isolated perfused rat lungs, some of which were subjected to acute oxidant lung injury. Both injured and control lungs were perfused with solutions containing heterologous fibronectin. The technique clearly demonstrated differences in the amount of tissue fibronectin in injured and noninjured lung as well as differences between lungs exposed to fibronectin and those not exposed. The described technique offers a reliable method for quantifying tissue fibronectin and is sensitive enough to detect differences in tissue fibronectin under experimental conditions of acute lung injury.

Fibronectin (FN) is a large dimeric glycoprotein with a molecular weight of about 440,000. The dimer is composed of two subunits, mol wt 200,000–250,000, joined by disulfide bonds at the extreme carboxyl terminal end (1). The FN molecule is composed of several structural domains with regions which bind to a number of moieties including collagen (2), heparin (3), actin (4), DNA (5), and *Staphylococcus aureus* (6). There is also a region which interacts with cell surfaces, mediating cell adhesion (7). FN is found in a soluble form in human plasma in a concentration of 300 μg/ml (8) and in an insoluble form in basement membranes and extracellular matricial structures of most tissues (9).

Fibronectin probably functions as an adhesive protein mediating cell-to-cell (10) and cell-to-substrate (11–13) adhesion. The immunoelectron microscopic localization of FN to endothelial cell junctions, endothelial cell basal lamina, and the interstitial space (14) suggests that cellular FN may be crucial in maintaining the integrity of endothelial and epithelial barriers. The alveolar–capillary unit of the lung is an example of a structure whose integrity may be dependent upon intact FN. The demonstration, *in vitro,* of FN's susceptibility to degradation by neutral proteases released by neutrophils (15) suggests that such degradation *in vivo* could represent an important mechanism in the development of increased alveolar–capillary permeability seen in many forms of acute lung injury. Furthermore, the demonstration that human plasma FN, when administered intravenously to mice, is distributed in tissues in a pattern indistinguishable from native mouse tissue FN (16), suggests the possibility that plasma FN could restore depleted or degraded tissue FN. Such restoration could have a propitious effect on tissue integrity and organ function.

Current techniques for quantification of tissue FN (17, 18) require extraction of FN from the tissue and therefore give no information about the its distribution in the tissue. We have used a technique combining peroxidase–antiperoxidase (PAP) immunocytochemistry and automated scanning light microscopy to quantify the changes in lung FN in isolated perfused lungs subjected to oxidant injury.

Our results indicate that (i) this technique can be used to quantify FN in lung tissue, (ii) FN was released from the lung tissue after oxidant injury and, (iii) exogenous plasma FN was taken up with increased avidity by the injured lung tissue when compared to controls.

Materials and Methods. *Animals and surgical procedures.* An isolated perfused rat lung model was used. Male Sprague–Dawley rats, weighing 250–300 g, were anesthetized with 7.2% chloral hydrate (1 cc/100 g) intraperitoneally and anticoagulated with 1000 units of intravenous heparin. The trachea

0037-9727/88 $1.50

was cannulated and animals were ventilated with a Harvard volume ventilator at a tidal volume of 1 cc/100 g, a rate of 60 breaths/min, and a positive end expiratory pressure of 2 cm H_2O. The heart, lungs, and abdominal cavity were exposed by a midline ventral incision and the abdominal aorta and inferior vena cava were severed. The heart was transected through the right and left ventricles and a catheter, primed with perfusate, was secured in the pulmonary artery. The left atrium was then severed. The trachea and lungs were removed and hung in a humidified 37°C chamber. Perfusate was continuously recirculated from a 200-ml reservoir. The lungs were perfused with warmed (37°C), preoxygenated buffered Krebs–Ringer solution (0.1% β-D-glucose, 4.5% bovine serum albumin), at a rate of 20 ml/min. The bovine serum albumin used (Sigma Chemical Co., A7906) was free of FN contamination, as determined by ELISA. Pulmonary artery pressures, airway pressures, and lung weights were continuously measured and recorded.

The perfused lungs were treated in one of four ways:

(i) Group I (control) (n = 3). Lungs were perfused for 60 min with Krebs–Ringer buffer solution only.

(ii) Group II (oxidant injury) (n = 7). After a 15-min baseline period, 1 mg of glucose oxidase was added to the perfusate. Perfusion was continued until lung weights reached twice the baseline value.

(iii) Group III (control + FN) (n = 5). Lungs were perfused as in the control group. Human plasma FN (Revlon, Yonkers, NY) was added to the perfusate at 15 min to achieve a final concentration of 200 μg/ml. Perfusion was continued for a total of 60 min.

(iv) Group IV (oxidant injury + FN) (n = 10). Lungs were treated as in the oxidant injury group. However, the oxidant reaction was stopped after lung weights were increased by 15% over baseline values by adding 1 mg catalase in 0.01 M phosphate-buffered normal saline (PBS, pH 7.0–7.2) to 200 ml perfusate. Human plasma FN was then added to the perfusate to yield a final concentration of 200 μg/ml. Perfusion continued until lung weights reached twice baseline values.

Tissue preparation. Lungs from the four groups were fixed by pulmonary arterial perfusion with 96% ethanol at 4°C followed by immersion in 96% ethanol at 4°C. Two transverse cuts were made through the right lateral lobe and the left lobe of the fixed lung tissue, and the samples were left in fixative for an additional 12 to 24 hr at 4°C. Tissues were dehydrated in two 1-hr changes of 100% ethanol followed by two 1-hr changes in xylene. Tissues were infiltrated with paraffin (Surgipath Medical Industries, Inc., Grayslake, IL) with a melting point of 56–57°C for 1 hr at ambient pressure, followed by infiltration with the same paraffin in a vacuum (20 mm Hg) for ½ hr. Tissues were embedded in paraffin and tissue blocks stored at −20°C until sectioning. Six-micrometer-thick sections were cut and floated on a 40°C waterbath for 30 sec before being picked up on gelatin-coated slides. Slides were air dried and stored at −20°C until processed for immunocytochemistry. Slides were deparaffinized in two 5-min changes in xylene, followed by two 5-min changes in 100% ethanol, two 5-min changes in 95% ethanol, one 5-min change in 70% ethanol, and a distilled water rinse. Slides were placed in a bath of 0.3% hydrogen peroxide in methanol for 30 min to eliminate endogenous peroxidase activity and were then rinsed in distilled water and three 10-min changes in PBS.

Staining. After dewaxing and rehydration, sections were processed for immunocytochemistry using the peroxidase–antiperoxidase technique (19). Affinity purified rabbit anti-human plasma FN IgG, 1 mg/ml (kindly supplied by Dr. John A. McDonald, Jewish Hospital, St. Louis, MO), was diluted 1:350 in 0.01 M PBS and gently pipetted over tissue sections. Slides were incubated at room temperature in a humidity chamber overnight and then rinsed in three 5-min washes of PBS. Excess PBS was blotted from all areas of the slide except the area containing the tissue. Affinity purified goat anti-rabbit IgG, 4 mg/ml (Miles Scientific, Naperville, IL), was diluted 1:100 in PBS and applied to sections in the same manner; sections were incubated at 37°C for 1 hr in a

humidity chamber followed by three 5-min rinses in PBS. Rabbit PAP complex was diluted 1:200 in PBS and applied to sections which were incubated in a humidity chamber for 30 min at 37°C and rinsed in three 5-min washes of PBS. Peroxidase labeling was demonstrated by incubating sections in a fresh filtered solution of 0.05% diaminobenzidine (DAB, Sigma Chemical Co.) with 0.001% hydrogen peroxide for 10 min, followed by a distilled water rinse. The positive reaction product formed by the peroxidase reaction with DAB was recognized as a light to dark brown color. Slides were not counterstained. Sections were dehydrated in graded alcohols and xylene and mounted in Permount. All slides used for final data analysis were processed in the same batch, which also contained immunocytochemistry control slides.

Controls for the immunocytochemistry included (i) anti-FN antiserum preabsorbed with 300 μg of antigen per milliliter of diluted serum; (ii) PBS substituted for the first-layer antiserum; (iii) PBS substituted for second-layer antiserum; (iv) PBS substituted for the PAP complex; (v) purified preimmune rabbit IgG substituted for the first-layer antiserum at a dilution of 1:350 in PBS. No specific staining was observed with any controls. The absence of staining on basement membrane or cells with the preabsorbed serum demonstrated that the anti-FN antibody was specific for FN.

Photometry. All samples were analyzed using a Zeiss Universal research microscope (Carl Zeiss, Inc., Thornwood, NY), equipped with a stabilized high-voltage power supply, photometer head, and a Hamamatsu photomultiplier tube (PMT; R928) which covers the range between 185 and 930 nm. The light source was a 100-W tungsten halogen lamp. The system was interfaced with a Zonax programmable microcomputer. The area of the specimen illuminated by the light source was controlled by the choice of an appropriate aperture size, and diaphragms determined the size of the area being measured.

Immunoreactivity to FN was quantified with an automatic scanning program (Bioscan, Carl Zeiss, Inc.). In this mode, the highest intensity values are selected and set automatically by the software program at 100% transmitted light. Amplifier gain and high-voltage values are automatically controlled by the computer as are the manipulations of the microscope shutters and diaphragms. The photometry readings ranged from 0% intensity (total darkness) to 100% intensity (bright light). The DAB reaction product was seen as a brown color, the more intense the reaction, the darker the color. The light intensity measured by the photometer was determined by the amount of light passing through the specimen. The amount of FN reactivity was directly related to the density of the reaction product, and inversely to the amount of light transmitted. One homogeneous sample area of parenchyma, 0.5 mm^2 per section, free of large airways or vascular structures, was chosen for scanning. A measuring field diameter of 1 μm was calculated using a 40X objective, 1.25 tube factor, and 0.05-mm measuring diaphragm diameter. A total of 1024 point measurements was made per slide, with 22 μm between measurements. The preabsorption staining control slide was similarly scanned.

To determine which intensity values represented FN immunoreactivity, random lung tissue samples from each group were chosen and quantified using the manual mode. In this mode, the operator selects the levels of signal amplification by amplifier gain and high-voltage settings based on the available light. A sample was first scanned using the automatic scanning program. The values for signal amplification and high voltage were calculated by the computer in the automatic mode and displayed on the computer cathode ray screen. These values were then used to obtain the readings in the manual mode. The manual mode readings for the sample were always done immediately after the automatic readings for the same sample. In this way, there was less possibility of introducing errors such as variations in light intensity and random fluctuations in operator technical ability.

For the manual mode samples, the entire section was scanned and 50 point readings were made, choosing only those points visually determined to have the darkest PAP staining and to have unquestionable FN positive immunoreactivity. These readings were then used to determine which range of

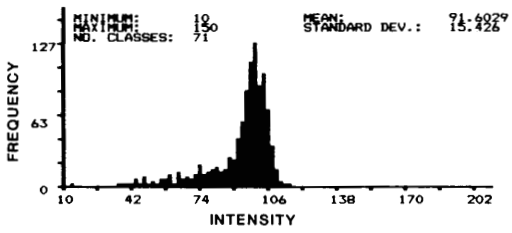

FIG. 1. A representative computer generated histogram depicting the results of an automatically scanned section of uninjured control lung (Group I).

density values represented FN immunoreactivity.

When scanning of a specimen was completed, the data obtained were displayed using a histogram program (Fig. 1). A fixed X axis which displayed the intensity range on a linear scale with intervals of two intensities was used. The maximum frequency of the data points was displayed on the Y axis. A class listing giving the exact frequency of the data in a chosen interval and the relative percentage of the frequency in each interval was obtained.

Statistical analysis. The χ^2 test or paired t test was used to determine statistical significance, set at $P < 0.05$.

Results. *Physiologic data.* Lungs from Groups I and III, those perfused with Krebs–Ringer buffer solution only, showed no changes in weight, pulmonary artery pressure, or airway pressure during the course of the perfusion.

Lungs from Groups II and IV, those exposed to high-energy oxygen species generated by the glucose–glucose oxidase reaction, developed pulmonary edema, manifest by significant increases in airway pressure, pulmonary artery pressure, and lung weight. There were no significant differences between Groups II and IV.

Light microscopy. Group I (control). The architecture of the lungs in this group was normal. Reaction product was seen at the luminal surfaces of the alveoli and around capillaries (Fig. 2).

Group II (oxidant injury). The architecture of the lungs in this group was slightly distorted. Several areas with dilated lobules were noted. Individual alveolar walls remained fine and delicate. The staining reac-

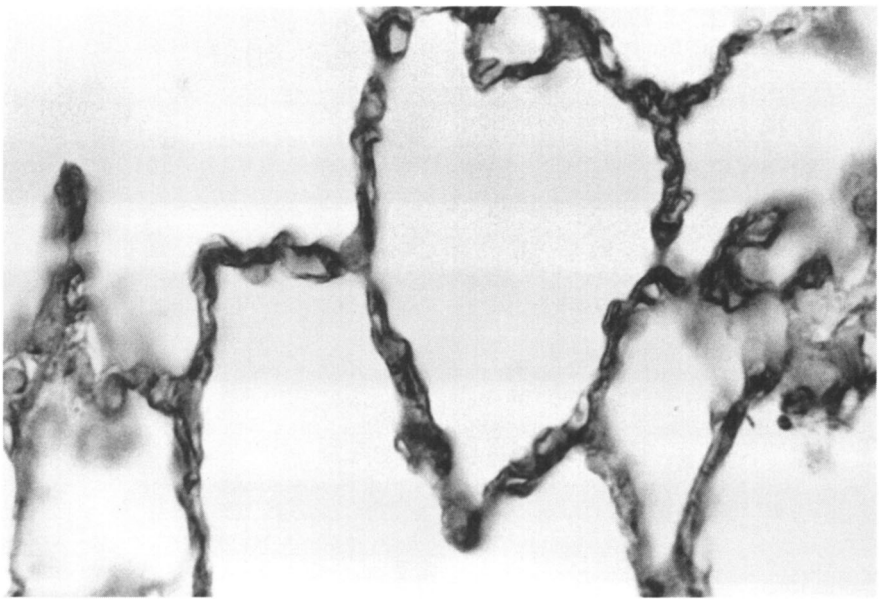

FIG. 2. Group I (control): antifibronectin–PAP-treated section showing FN positive immunoreactivity at the luminal surface and around capillaries. ×800.

tion of these samples was generally weaker than that of the controls. Many alveolar septa showed no positive staining. Some alveoli showed no positively stained capillaries (Fig. 3).

Group III (control + FN). In this group, normal lung architecture was preserved. The FN positive staining pattern was similar to that in controls, but more intense. Most capillaries were outlined with FN positive staining. The region of the basement membrane showed intense immunoreactivity (Fig. 4).

Group IV (oxidant injury + FN). Lung architecture in this group was also slightly distorted with few distended lobules noted. This group showed the most intense staining reaction. Strong reactions were seen outlining capillaries and the area of the basement membrane (Fig. 5).

Analysis of FN immunoreactivity. The computer software program generated a listing of intensity readings as well as histograms for each section analyzed. Using the values obtained from the manually scanned samples, we determined that the darkest PAP staining had transmission values ≦60%. This was considered unquestionable FN staining.

The 1024 intensity readings from each sample were broken down into classes representing transmission values in the ranges ≦40%, 41–60%, 61–80%, 81–100%, and ≧101%. The total number of readings within each range was then calculated for each sample. All of the data for each treatment group were then pooled. Figure 6 illustrates the mean and standard error for the number of intensity readings that fell within the chosen ranges. The composite data for each group are represented in histogram form.

All intensity values recorded for the preabsorption staining control slide were in the >61% range, indicating no FN positive readings.

In Group I (control) the majority of FN positive values were within the 41–60% range with a few falling in the ≦40% range.

Oxidant injury of the lungs in Group II resulted in fewer intensity readings in the ≦40% range and no significant change in the 41–60% ranges compared with uninjured controls, suggesting a loss of FN.

The uninjured lungs which were exposed to exogenous FN (Group III) showed an obvious increase in the number of FN positive readings in both the ≦40% and the 41–60% ranges compared with uninjured controls.

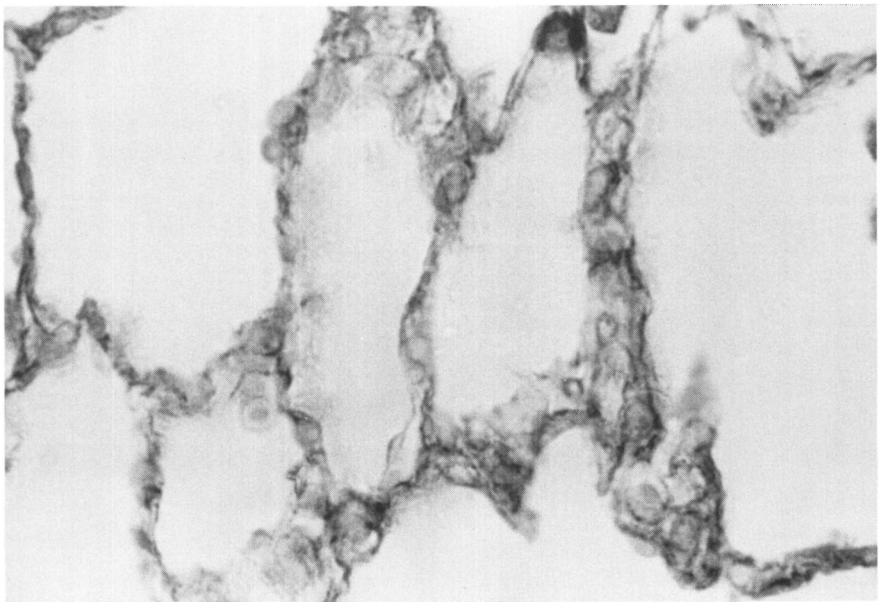

FIG. 3. Group II (oxidant injury): antifibronectin–PAP-treated section of oxidant injured lung tissue. FN positive immunoreactivity is generally weaker than that of Group I controls. ×800.

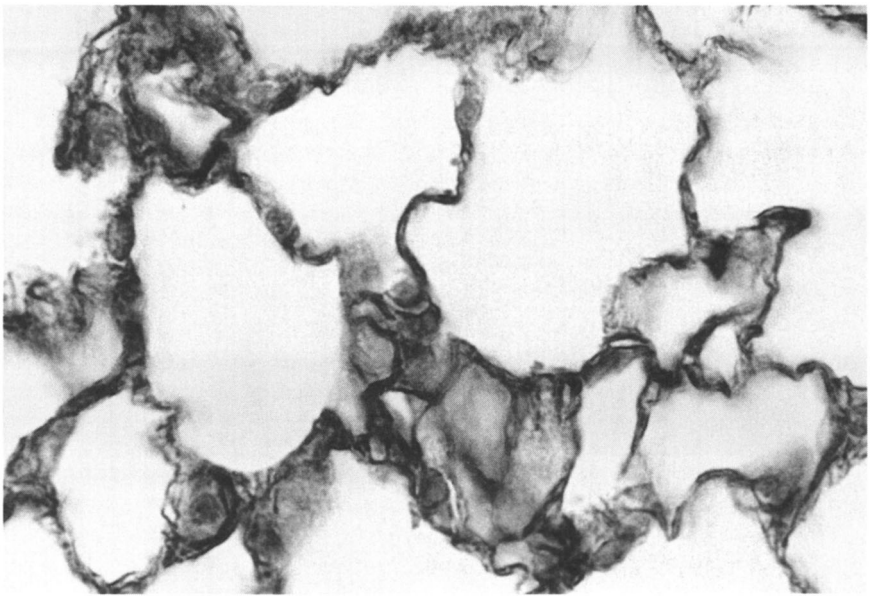

FIG. 4. Group III (control + FN): antifibronectin–PAP-treated section showing the distribution of FN positive immunoreactivity to be similar to but more intense than that in Group I controls. ×800.

Oxidant injured lungs exposed to exogenous FN (Group IV) showed a marked increase in the number of FN positive readings in both the ≦40% and the 41–60% ranges compared with the uninjured controls (Group I) and the uninjured lungs exposed to FN (Group III).

All treatment groups were compared to the

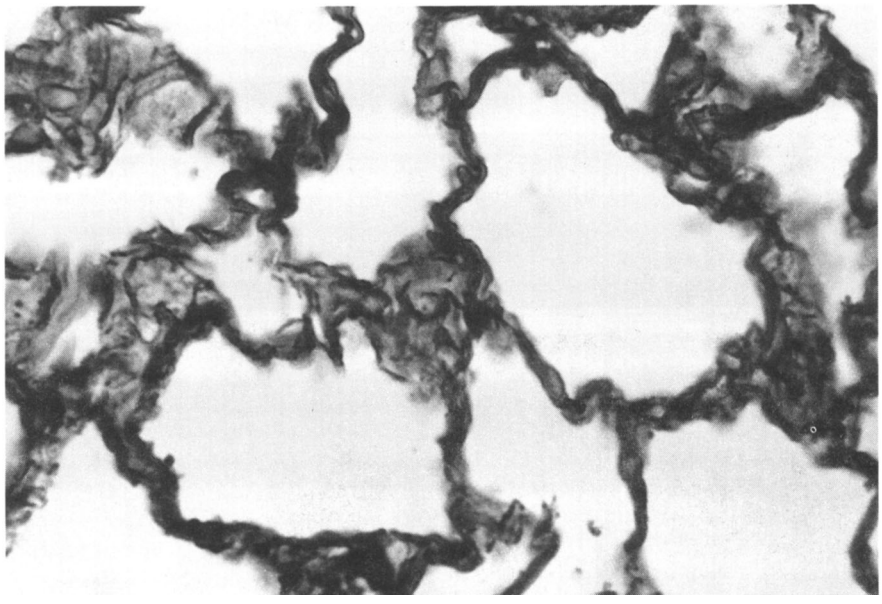

FIG. 5. Group IV (oxidant injury + FN): antifibronectin–PAP-treated section showing the most intense FN positive immunoreactivity of all groups. ×800.

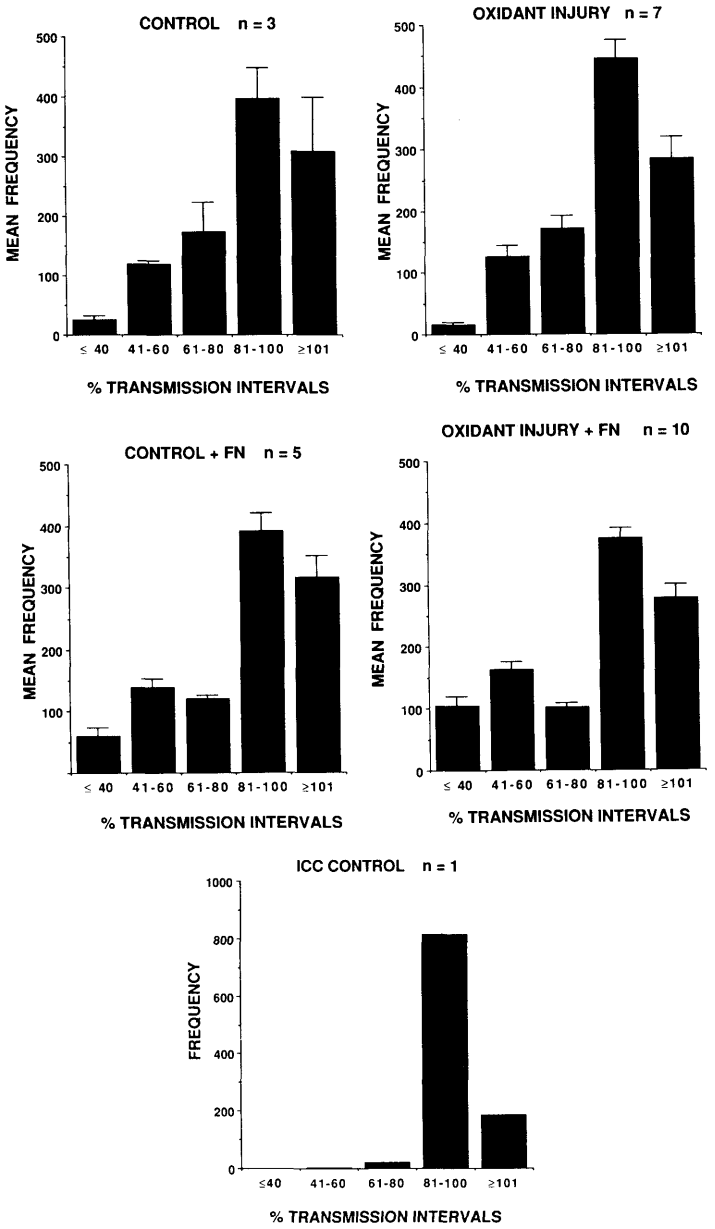

FIG. 6. Frequency data are means (±SE) of all intensity readings from all animals in each group. Intervals were selected on the basis of χ^2 analysis using the manually determined range for FN positive readings. A preabsorbed control histogram has been included to demonstrate the specificity of FN positive immunoreactivity.

uninjured control group, and the control + FN group was compared to the oxidant injury + FN group. All groups were found to be significantly different ($P < 0.05$).

Discussion. We have described a method for the quantification of FN in lung tissue using a combination of immunocytochemistry and computerized light microscopy. Prior studies have used immunohistochemical and immunofluorescent methods to describe the distribution of tissue FN. Stenman and Vaheri (9), using immunofluorescence, demon-

strated FN in loose connective tissue, around fat, skeletal muscle, and smooth muscle cells, and in association with vascular and epithelial basement membranes. Kurkinen *et al.* (20) were able to detect FN deposition during granulation tissue formation. Rosenkrans *et al.* (21) described the distribution of FN in the developing rat lung using immunocytochemistry, and Du Boulay (22) demonstrated that FN was present in several human soft tissue tumors using similar techniques. While these studies depended on qualitative methodologies, the technique described in the current study offers the advantage of yielding both qualitative and quantitative information about FN distribution in tissues.

The staining patterns we observed are consistent with those of other studies involving lung tissue. Bray (18) was able to detect FN biochemically in alveolar basement membrane which was solubilized by enzymatic digestion and reacted with anti-FN antiserum. Stenman and Vaheri (9), using immunofluorescence, localized FN in alveolar walls around capillaries and basement membrane of alveolar epithelium, as well as in basement membrane of trachea and bronchi. Torikata *et al.* (14) compared the distribution of FN in normal and fibrotic human lung using anti-FN Fab′–horseradish peroxidase conjugates. Light microscopy in normal lung showed that bronchiolar and alveolar epithelium, smooth muscle, and endothelial basement membranes all stained for FN. Corresponding ultrastructural studies of the normal lung showed that basal lamina was the most heavily stained matrix structure. Rosenkrans *et al.* (21), using the PAP method, found FN associated with the basal lamina and alveolar surface of the adult rat lung.

The peroxidase–antiperoxidase and immunofluorescence methods yield nearly identical quantitative results in studies using various tissue antigens (23, 24). Miller *et al.* have described an immunofluorescent technique for quantification of collagen in irradiated mouse lung (25). We chose to use the PAP method because it allowed for conventional light microscopic evaluation, permitting a simultaneous study of morphology (24). In addition, the PAP method yields a resolution of intracellular staining superior to that of the fluorescent antibody staining method (23). Furthermore, the PAP method results in an end product which is stable and not subject to photobleaching error inherent to fluorescent staining (23).

Use of the automatic scanning program made it possible to scan a homogeneous, precisely defined area within each section of lung tissue. Each section was scanned in the same manner and the same number of point readings was obtained for each section. Automatic scanning also permitted many more point readings than would be practical with manual techniques. Because homogeneity was a major criterion for choosing the area of the section to be scanned, it was impossible to always choose the same portion of lung tissue for scanning.

The 0.05-mm-diameter scanning diaphragm permitted homogeneous point readings to be made in the manual mode. A single FN-immunoreactive cell could completely fill the opening. This small aperture size was necessary in order to ensure that incorrect measurements were not made when establishing the range of FN positive readings. That is, in establishing the range of FN positive readings, we did not wish to measure an area containing both air and a FN-immunoreactive cell. The small aperture also minimized incorrect measurements in the automatic mode.

The ethanol tissue fixation and PAP method of tissue staining afforded clean sample staining with little nonspecific background staining. Chemnitz and Christensen (26) compared immunoperoxidase staining for FN in ethanol and formaldehyde fixed normal and healing arterial tissue. They found that ethanol-fixed tissue consistently showed moderate to strong staining intensity, while formaldehyde-fixed tissue required proteolytic digestion before the same staining intensity was seen. Szendroi *et al.* (27) compared several fixatives and immunohistochemical methods for the detection of FN in various paraffin-embedded tissues. They found that 96% ethanol-fixed tissues resulted in the strongest staining intensity.

Our experimental design was based upon the likelihood that partially reduced oxygen species could directly damage FN, resulting in a loss of FN or FN antigenicity from the

tissue, or that loss of tissue FN could also be caused by oxidant damage to other cellular or matricial components (28). We did find that lungs subjected to oxidant injury (Group II) demonstrated significantly less FN staining than uninjured lungs (Group I). This result is consistent with, and complementary to, data recently reported by Peters *et al.*, who described release of tissue FN from *in vitro* perfused rabbit lung subjected to oxidant injury (29). By measuring perfusate FN concentrations, these authors found that oxidant injured lungs released increased amounts of FN. Additionally, they demonstrated that this FN was intact and dimeric and composed of subunits with electrophoretic mobility similar to that of FN extracted from normal human lung tissue. In contrast, FN recovered from lungs treated with trypsin-containing perfusate contained FN cleavage products. While Peters *et al.* suggested that the release of intact tissue FN might be from oxidant stressed endothelial cells, our findings imply a more widespread loss of tissue FN.

When the pulmonary circulation of noninjured lungs (Group III) was perfused with a solution containing heterologous plasma FN, there was a relatively homogeneous uptake of FN, similar to that noted by Oh *et al.* (16) *in vivo*. Lungs subject to oxidant injury before perfusion with FN-containing solution (Group IV) showed a marked increase in FN staining compared with uninjured, FN exposed lungs. Several possible explanations exist for the increased tissue uptake of FN after tissue injury. Damage to lung tissue basement membrane by oxygen radicals may have resulted in the exposure of additional FN binding sites. Other possible sources of increased FN binding sites include injured endothelial and epithelial cell membranes or binding sites newly exposed when cells are separated from each other or their basement membranes. Alternatively, the increased uptake of FN may simply be a reflection of interstitial trapping of FN under conditions of increased transcapillary flux of water and solute during oxidant induced pulmonary edema. In comparing perfused versus nonperfused rat kidney sections, Courtoy and Boyles (30) concluded that "the distribution of fibronectin is largely obscured in nonperfused tissue by significant amounts of plasma CIG loosely trapped in the extracellular matrix." The notion of nonspecific interstitial trapping of FN in the lung is a plausible but untested hypothesis.

In conclusion, we have shown that tissue FN immunoreactivity can be quantified with a technique combining immunocytochemistry and scanning light microscopy. This technique was used to show that oxidative lung injury results in a loss of tissue FN. Furthermore, after oxidative lung injury, the injured lung tissue avidly takes up perfused plasma FN by a mechanism that has yet to be elucidated. The physiologic implications of these findings, specifically in regard to the role of tissue FN in the pathogenesis of acute lung injury, remain unclear.

This study was supported, in part, by grants from the American Lung Association of Wisconsin and the Revlon Health Care Group. The authors thank Adriane Rademakers for her technical assistance with collection and preparation of samples for immunocytochemical evaluation. We also thank Dr. Julian Messina, Dr. James Sehloff, and Ms. Laura Stein for their assistance during the study.

1. Mosher DF. Fibronectin. Prog Hemostasis Thromb **5**:111–151, 1980.
2. Engvall E, Ruoslahti E, Miller EJ. Affinity of fibronectin to collagens of different genetic types and to fibronectin. J Exp Med **147**:1584–1595, 1978.
3. Petersen TE, Thogersen HC, Skorstengaard K, Vibe-Pedersen K, Sahl P, Sottrup-Jensen L, Magnusson S. Partial primary structure of bovine plasma fibronectin: Three types of internal homology. Proc Natl Acad Sci USA **80**:137–141, 1983.
4. Keski-Oja J, Sen A, Todaro GJ. Direct association of fibronectin and actin molecules in vitro. J Cell Biol **85**:527–533, 1980.
5. Zardi L, Siri A, Carnemolla B, Santi L. Fibronectin: A chromatin-associated protein? Cell **18**:649–657, 1979.
6. Mosher DF, Proctor RA. Binding and factor XIIIa-mediated cross-linking of a 27-kilodalton fragment of fibronectin to *Staphylococcus aureus*. Science **209**:927–929, 1980.
7. Pierschbacher MD, Hayman EG, Ruoslahti E. Location of the cell-attachment site in fibronectin with monoclonal antibodies and proteolytic fragments of the molecule. Cell **26**:259–267, 1981.
8. Mosesson MW, Umfleet RA. The cold-insoluble globulin of human plasma. I. Purification, primary characterization, and relationship to fibrinogen and

other cold-insoluble fraction components. J Biol Chem **245**:5728–5736, 1970.
9. Stenman S, Vaheri A. Distribution of a major connective tissue protein, fibronectin, in normal human tissues. J Exp Med **147**:1054–1064, 1978.
10. Yamada KM, Yamada SS, Pastan I. The major cell surface glycoprotein of chick embryo fibroblasts is an agglutinin. Proc Natl Acad Sci USA **72**:3158–3162, 1975.
11. Klebe JR. Cell attachment to collagen: The requirement for energy. J Cell Physiol **86**:231–236, 1975.
12. Pearlstein E. Plasma membrane glycoprotein which mediates adhesion of fibroblasts to collagen. Nature (London) **262**:497–500, 1976.
13. Hynes RO, Ali IU, Destree AT, Mautner V, Perkins ME, Senger DR, Wagner DD, Smith KK. A large glycoprotein lost from the surfaces of transformed cells. Ann NY Acad Sci **312**:317–342, 1978.
14. Torikata C, Villiger B, Kuhn C III, McDonald JA. Ultrastructural distribution of fibronectin in normal and fibrotic human lung. Lab Invest **52**:399–408, 1985.
15. McDonald JA, Baum BJ, Rosenberg DM, Kelman JA, Brin SC, Crystal RG. Destruction of a major extracellular adhesive glycoprotein (fibronectin) of human fibroblasts by neutral proteases from polymorphonuclear leukocyte granules. Lab Invest **40**:350–357, 1979.
16. Oh E, Pierschbacher M, Ruoslahti E. Deposition of plasma fibronectin in tissues. Proc Natl Acad Sci USA **78**:3218–3221, 1981.
17. Rosenkrans WA, Penney DP. Cell–cell matrix interactions in induced lung injury. Radiat Res **109**:127–142, 1987.
18. Bray BA. Presence of fibronectin in basement membranes and acidic structural glycoproteins from human placenta and lung. Ann NY Acad Sci **312**:142–150, 1978.
19. Sternberger LA. Immunocytochemistry. New York, Wiley, 2nd ed. 1979.
20. Kurkinen M, Vaheri A, Roberts PJ, Stenman S. Sequential appearance of fibronectin and collagen in experimental granulation tissue. Lab Invest **43**:47–51, 1980.
21. Rosenkrans WA Jr, Albright JT, Hausman RE, Penney DP. Ultrastructural immunocytochemical localization of fibronectin in the developing rat lung. Cell Tissue Res **234**:165–177, 1983.
22. Du Boulay CEH. Demonstration of fibronectin in soft tissue tumours using the immunoperoxidase technique. Diagn Histopathol **5**:283–289, 1982.
23. Smith MT, Redick JA, Baron J. Quantitative immunohistochemistry: A comparison of microdensitometric analysis of unlabeled antibody peroxidase–antiperoxidase staining and of microfluorometric analysis of indirect fluorescent antibody staining for nicotinamide adenosine dinucleotide phosphate (NADPH)-cytochrome *c* (*P*-450) reductase in rat liver. J Histochem Cytochem **31**:1183–1189, 1983.
24. Valnes K, Brandtzaeg P, Hanssen LE, Stave R, Larsen S, Londong W. Quantitation of immunoglobulin- and peptide hormone-producing cells in gastrointestinal mucosa. Comparison of direct immunofluorescence and the unlabelled antibody peroxidase–antiperoxidase method. Histochem J **15**:1011–1020, 1983.
25. Miller G, Sieman D, Scott P, Dawson D, Muldrew K, Trepanier P, McGann L. A semiquantitative probe for radiation-induced normal tissue damage at the molecular level. Radiat Res **105**:76–83, 1986.
26. Chemnitz J, Christensen BC. Repair in arterial tissue. Demonstration of fibronectin in the normal and healing rabbit thoracic aorta by the indirect immunoperoxidase technique. Virchows Arch (Pathol Anat) **399**:307–316, 1983.
27. Szendroi M, Labat-Robert J, Godeau G, Robert AM. Immunohistochemical detection of fibronectin using different fixatives in paraffin embedded sections. Pathol Biol **31**:631–636, 1983.
28. Bishop CT, Freeman BA, Crapo JD. Free radicals in lung injury. In: Armstrong D, Sokal R, Cutler RG, Slater TF, Eds. Free Radicals in Molecular Biology, Aging and Disease. New York, Raven Press, 1st ed., pp 381–390, 1984.
29. Peters JH, Ginsberg MH, Bohl BP, Sklar LA, Cochrane CG. Intravascular release of intact cellular fibronectin during oxidant-induced injury in the in vitro perfused rabbit lung. J Clin Invest **78**:1596–1603, 1986.
30. Courtoy PJ, Boyles J. Fibronectin in the microvasculature: Localization in the pericyte–endothelial interstitium. J Ultrastruct Res **82**:258–273, 1983.

Received April 23, 1987. P. S. E. B. M. 1988, Vol. 188.
Accepted February 8, 1988.